Meteorologische Zeitschrift, Vol. **15**, No. 2, 147-156 (April 2006)

Article

Dynamical processes related to cyclone development near Greenland

RAGNHILD BIELTVEDT SKEIE[1], JÓN EGILL KRISTJÁNSSON*[1], HARALDUR ÓLAFSSON[2,3] and BJØRN RØSTING[4]

[1]Department of Geosciences, University of Oslo, Oslo, Norway
[2]Icelandic Meteorological Office, Reykjavik, Iceland
[3]University of Iceland and Institute for Meteorological Research, Reykjavik, Iceland
[4] Norwegian Meteorological Institute, Oslo, Norway

(Manuscript received July 31, 2005; in revised form September 27, 2005; accepted September 30, 2005)

Abstract

An unusual cyclone that moved over Greenland and caused blizzard conditions over eastern Greenland and northern Iceland on 20–21 September 2003 is investigated. Numerical simulations are conducted to assess the role of Greenland's orography for the development, as well as to evaluate the significance of other factors such as latent heating and sea surface temperature (SST). The simulations reveal that the cyclone evolution was crucially dependent on an interaction between the background flow and the orography of Greenland. When the orography is removed, a deep, well organized baroclinic low develops rapidly and moves eastward at 75°N. Conversely, in the control run, which is similar to the analyses, the evolution of the (primary) baroclinic low is greatly suppressed by the orographic retardation of the warm air ahead of and the cold air behind the low. Instead, a secondary low developing off Greenland's east coast at 68°N intensifies due to a coupling between an approaching upper level PV-anomaly and a lower level PV-anomaly generated from lee effects. This secondary low, absent in the run without orography, then moves eastward and causes the extreme weather conditions that were observed. Inversion of selected potential vorticity anomalies lends support to the above explanation. Further sensitivity experiments show that latent heating contributes about half of the deepening of the low, while SST amounts contribute much less.

Zusammenfassung

Es wird ein außergewöhnliches Tiefdruckgebiet, das über Grönland zog und am 20. und 21. Oktober 2003 einen schweren Schneesturm über Ost-Grönland und Nord-Island verursachte, untersucht. Numerische Simulationen werden durchgeführt, sowohl um die Rolle des grönländischen Gebirges als auch die Bedeutung weiterer Faktoren wie die Freisetzung latenter Wärme und die Meeresoberflächentemperatur zu analysieren. Diese Simulationen zeigen, dass die Entwicklung des Tiefdruckgebiets entscheidend von der Wechselwirkung zwischen der großräumigen Strömung mit dem grönländischen Gebirge abhing. Entfernt man das Gebirge, entwickelt sich rasch ein starkes, wohl organisiertes baroklines Tiefdruckgebiet, welches entlang des 75. Breitengrads ostwärts zieht. Im Gegensatz dazu ist die Entwicklung des primären baroklinen Tiefdruckgebiets im Kontrolllauf, der den Analysen ähnelt, weitgehend durch das Zurückhalten der Warmluft vor und der Kaltluft hinter dem Tief durch das Gebirge unterdrückt. Stattdessen intensiviert sich ein sekundäres Tief, das sich vor der grönländischen Küste bei 68°N gebildet hat, auf Grund einer Kopplung zwischen einer herannahenden PV-Anomalie in den höheren Schichten mit einer durch den Lee-Effekt erzeugten PV-Anomalie in den unteren Schichten. Dieses sekundäre Tiefdruckgebiet, welches in dem Lauf ohne Gebirge fehlt, bewegt sich dann ostwärts und verursacht die beobachteten extremen Wetterbedingungen. Eine Inversion von ausgewählten PV-Anomalien stützt die obige Erklärung. Sensitivitätsstudien zeigen weiterhin, dass die Freisetzung latenter Wärme ungefähr die Hälfte zur Vertiefung des Tiefs beiträgt, während die Höhe der Meeresoberflächentemperatur sehr viel weniger beiträgt.

1 Introduction

On 20 September 2003 explosive cyclogenesis off Greenland's east coast led to heavy snowfall and sustained winds exceeding 30 m/s over a 6 hour period at Illoqqortoormiut (70.5°N, 22.0°W) in Eastern Greenland, while the north coast of Iceland was hit by 15–25 m/s winds and wet snow the following day, as the low tracked eastwards. The purpose of this study is to investigate what role Greenland's orography and other factors may have played in the cyclone development, and to address these results in the context of other recent work on cyclones in the vicinity of Greenland.

In addition to being the largest island in the world, Greenland is also a major mountain range, with a plateau of over 3000 meters above sea level. The area between Greenland and Iceland has a lot of cyclone activity on various spatial and temporal scales, and it seems likely a priori that the orography of Greenland plays an impor-

*Corresponding author: Jón Egill Kristjánsson, Department of Geosciences, University of Oslo, P.O. Box 1022 Blindern, N-0315 Oslo, Norway, e-mail: j.e.kristjansson@geo.uio.no

0941-2948/2006/0114 $ 4.50

DOI: 10.1127/0941-2948/2006/0114

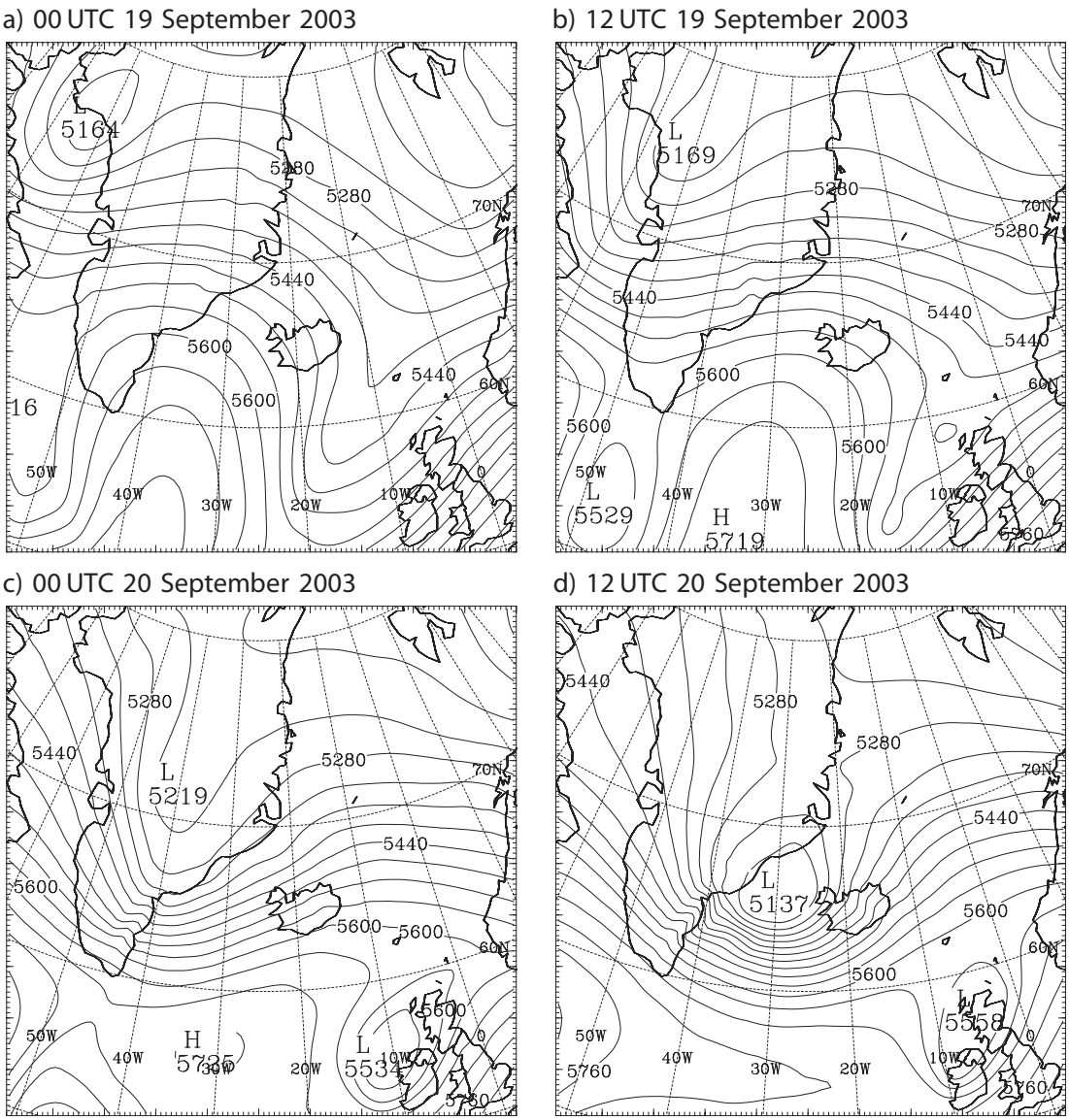

Figure 1: Geopotential height at 500 hPa [m] in the model analyses at a) 00 UTC 19 September 2003, b) 12 UTC 19 September 2003, c) 00 UTC 20 September 2003 and d) 12 UTC 20 September 2003.

tant role in this regard (SCORER, 1988). During the last few years the interest in how Greenland influences the atmospheric flow has grown. ÓLAFSSON (1998) demonstrated how crucial the horizontal resolution is for an adequate description of the flow around Greenland in numerical weather prediction models. KRISTJÁNSSON and MCINNES (1999) carried out a case study of a January 1995 cyclone developing between Greenland and Iceland. They found that the orography of Greenland suppressed the baroclinic development of the cyclone. Furthermore, a residual low between Iceland and Greenland was induced by orographic forcing. This result was supported by idealized simulations for westerly flow past simple mountains resembling Greenland by PETERSEN et al. (2003), who found a pressure deficit in the lee of southern Greenland, associated with transient eddies that repeatedly formed in this area. In a case study of a cyclone moving from the SW towards Ireland, they further found that an upper level lee trough SE of Greenland had a positive effect on the cyclone evolution due to a strengthening of the westerly baroclinic flow. Both SCHWIERZ and DAVIES (2003) and KURZ (2004) have described how Greenland's orography leads to a splitting of cyclones approaching from the south, with one low moving up the west coast and another forming off the southeast coast. PETERSEN et al. (2004) and more recently JUNGE et al. (2005) have studied the large-scale influences of Greenland on the Northern Hemisphere during winter using different global climate models and found that Greenland's orography not only pulls the Icelandic Low southwestwards, consistently with the findings of PETERSEN et al. (2003), but it also affects the flow patterns over North America and Asia.

On the mesoscale, it has been known for a long time that many coastal areas in Greenland exhibit strong katabatic winds. Recently, these winds were linked to the

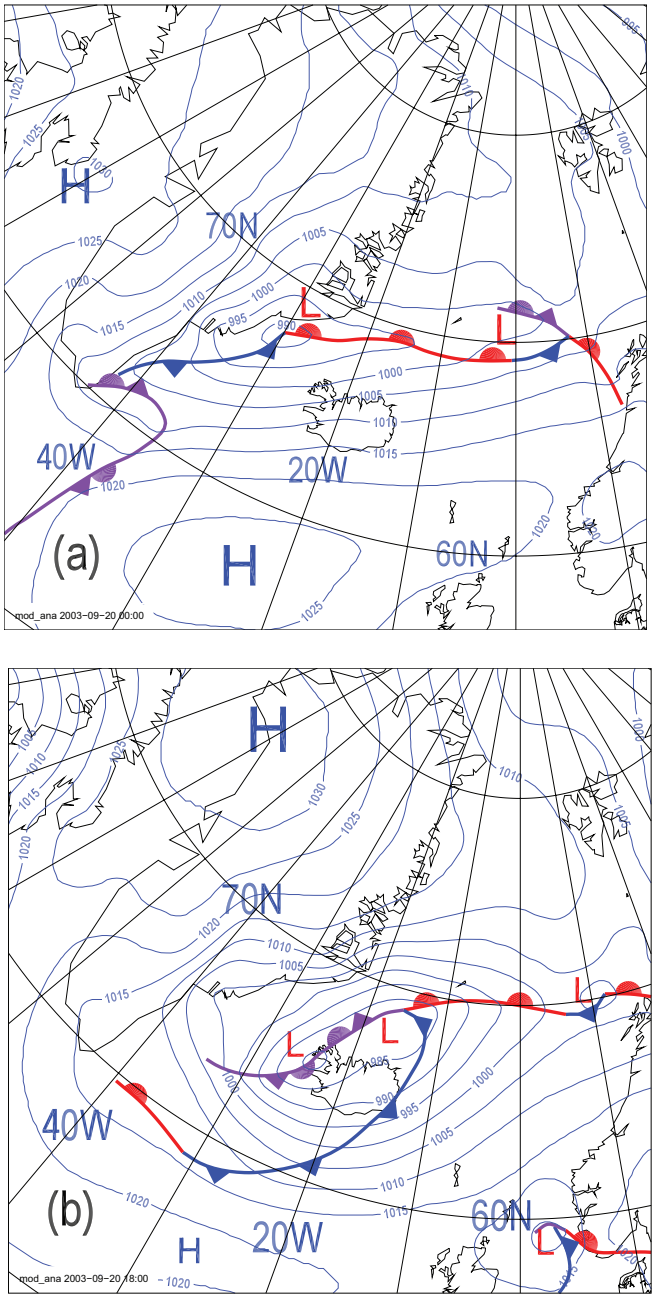

Figure 2: Subjective analysis of sea level pressure and fronts at a) 00 UTC 20 September 2003 and b) 18 UTC 20 September 2003.

occurrence of meso-cyclones off Greenland's east coast (KLEIN and HEINEMANN, 2002). There is a rising interest in the role of other mesoscale wind features such as tip jets (DOYLE and SHAPIRO, 1999), barrier winds (MOORE and RENFREW, 2005), and the possible significance of these phenomena for the vertical overturning in the adjacent ocean (PICKART et al., 2003).

In this study the 20 September 2003 case is simulated with the numerical model MM5, and sensitivity studies are carried out to evaluate the role of various factors such as Greenland's orography, latent heat and sea surface temperature (SST) for the cyclone evolution. The findings are then compared and related to recent work on the influence of Greenland on airflow, cited above. In section 4, inversion of selected potential vorticity anomalies is carried out, in order to quantitatively assess the importance of a proposed coupling between upper level forcing and the lower tropospheric development.

2 Model and simulations

The numerical model used in this study is the Pennsylvania State University-National Center for Atmospheric Research (PSU-NCAR) mesoscale model, MM5 (GRELL et al., 1995). The model has been run with a 36 km horizontal grid spacing and 100 x 100 grid points in the horizontal, while in the vertical there are 23 sigma layers. The integration domain, seen in e.g. Figure 3a, is centered at 68°N, 25°W. The following physical parameterization schemes were used: Grell cumulus parameterization scheme, MRF planetary boundary layer scheme, "simple ice" explicit moisture scheme and "cloud radiation" scheme (MM5 USER'S GUIDE, 2001). The initial and boundary conditions are derived from European Centre for Medium-Range Weather Forecast (ECMWF) analyses at T159 spectral truncation, and the lateral boundary conditions are updated every 6 hours. The model is run for 92 hours starting at 00 UTC 18 September 2003.

In addition to a control run with the standard model configuration (CONTROL), simulations have been carried out without mountains on Greenland (NOGREEN), without latent heat release (NOLAT) and with reduced sea surface temperature (REDSST). In the NOGREEN run the height of Greenland was set to 1 m, and the model extrapolated the initial conditions from the ECMWF analysis down to sea level. In the NOLAT run, the latent heat release was excluded from the parameterization schemes by turning off the temperature tendency arising from latent heating by condensation of water vapour in the thermodynamic energy equation. The REDSST run was conducted with the initial SST reduced by 5 K in the entire grid domain.

3 Synoptic description

On 18–19 September 2003, a slow-moving upper level trough was located over northwestern Greenland (Figures 1a,b). In the early hours of 20 September, this trough strengthened rapidly as it moved southeastwards (Figure 1c), reaching the Denmark Strait (67°N, 30°W) at 12 UTC 20 September (Figure 1d). At the surface, a weak disturbance moved from the northwest corner of Greenland toward the southeast on 18–19 September. Due to vortex shrinking over the mountainous terrain, this disturbance was almost absent in the lower troposphere, until it reached Greenland's east coast, whereupon a secondary low started to appear southwest of the

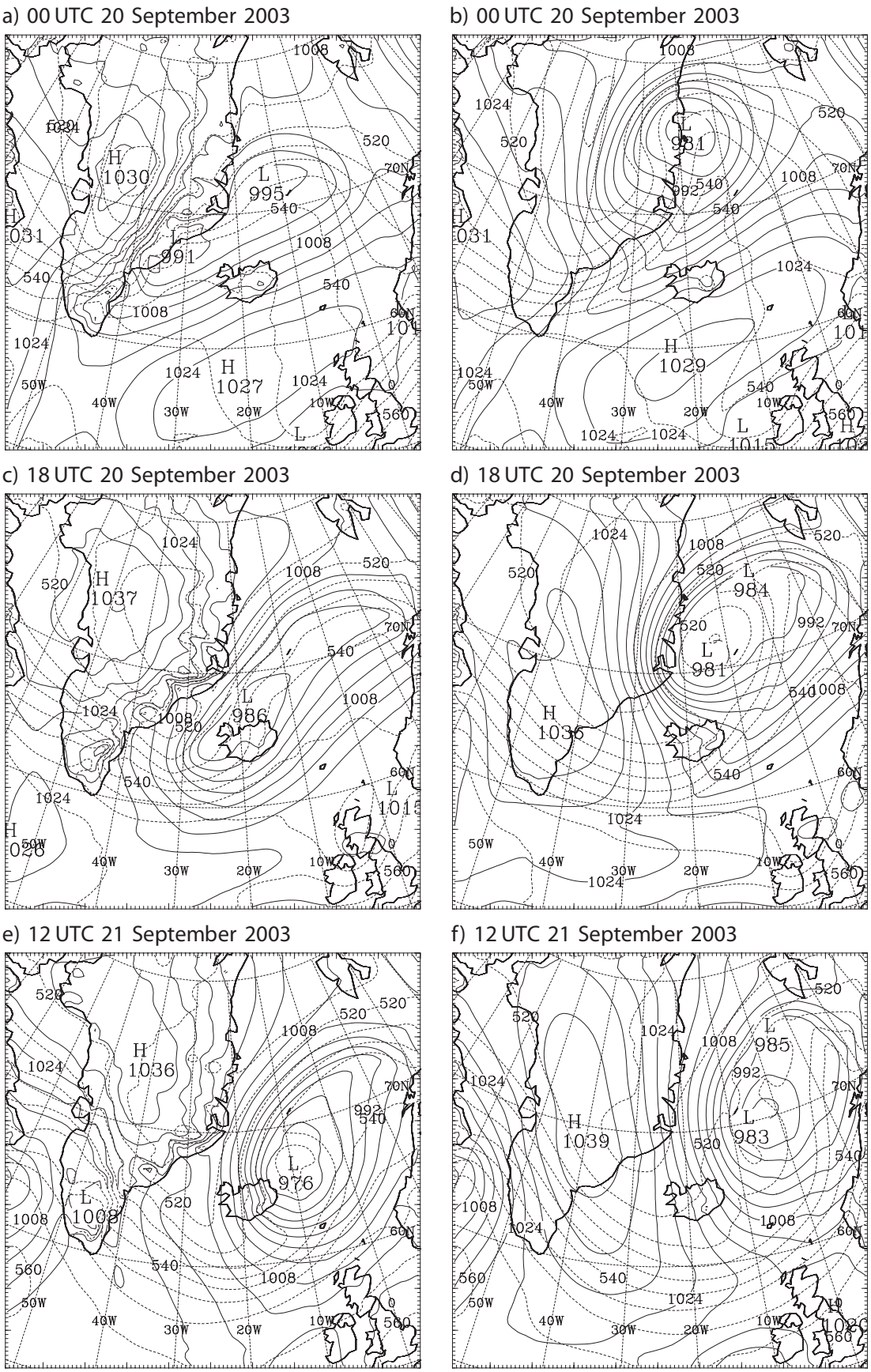

Figure 3: Sea level pressure [hPa, solid] and 500–1000 hPa thickness [m, dashed] in the CONTROL (left panel) and NOGREEN (right panel) simulations at +48 hours, 00 UTC 20 September 2003 (upper), +66 hours, 18 UTC 20 September 2003 (middle) and at +84 hours, 1200 UTC 21 September 2003 (lower).

Table 1: Central sea level pressure from the ECMWF analysis (ANALYSIS), in the CONTROL run, and relative to the CONTROL run in the four sensitivity experiments described in the text (units: hPa). For each simulation, the left column is for the primary low, the right column for the secondary low.

	ANALYSIS		CONTROL		NOGREEN	NOLAT		REDSST	
+36	1002	998	1000	989	–9	+5	+15	0	–1
+42	999	995	998	993	–12	+5	+12	0	0
+48		992	995	991	–14	+8	+11	+1	+2
+54		985	992	990	–13	+10	+7	+3	+2
+60		981	992	989	–10	+12	+8	+3	+2
+66		979		986			+10		+4
+72		980		982			+14		+3
+78		979		977			+16		+4
+84		978		976			+16		+5
+90		976		973			+18		+7
+96		974		974			+15		+6

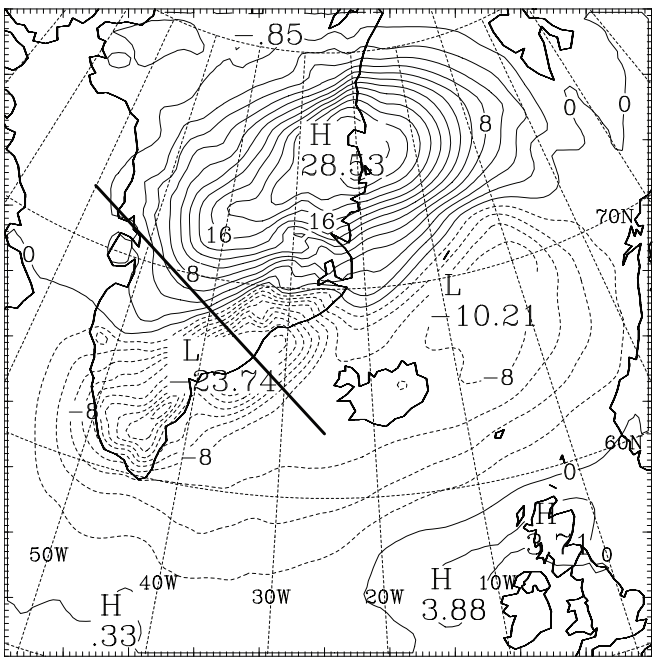

Figure 4: Sea level pressure difference [hPa] CONTROL minus NOGREEN at +48 hours, 00 UTC 20 September 2003. Solid line indicates location of cross sections in Figure 7.

primary baroclinic low. The interaction between the upper level trough and the secondary low is investigated in detail in the next section.

Figure 2a shows a subjective analysis at 00 UTC 20 September 2003, displaying the two surface disturbances, the rather weak baroclinic (primary) low just east of Jan Mayen island (71°N, 8°W) and a clearly developing secondary low off Greenland's east coast at 68°N, 30°W. During the following hours the secondary low intensifies, and simultaneously the primary baroclinic low weakens. Figure 2b shows the subjective analysis 18 hours later, at 18 UTC 20 September 2003. The secondary low has now become a major baroclinic disturbance, with associated winds exceeding 30 m/s at the eastern tip of Greenland, accompanied by dense snowfall, while the remnants of the primary low can be seen at 70° N, 10° E. The secondary low subsequently moved eastward, causing northerly gales, temperatures near freezing and heavy precipitation in northern Iceland on 21 September, due to a combination of frontal and orographic lifting of the air masses.

4 Main results

We will now show the results from the CONTROL and NOGREEN simulations, followed by a potential vorticity (PV) based interpretation.

4.1 Basic features

Figure 3a shows the sea level pressure at 00 UTC 20 September (+48 hours) from the CONTROL run. Compared to the subjective analysis (Figure 2a), the primary low is a few hPa deeper in the CONTROL simulation than in the analysis, and it is shifted westward by about 300 km. The secondary low is marginally weaker than in the analysis at this point, but the main features of this system are well captured in the CONTROL simulation. In the NOGREEN run, on the other hand, the secondary low is completely absent (Figure 3b), indicating that it is a lee low, as in KRISTJÁNSSON and MCINNES (1999). Furthermore, the evolution of the primary, baroclinic low is much more vigorous in NOGREEN than in the CONTROL run, as indicated in Table 1 and Figure 3b. Note for instance the strong cyclonic curvature around the well-developed cold front off Greenland's east coast, a feature that is missing in the CONTROL run. Due to the absence of any disrupting influences of Greenland's orography, the baroclinic low in this case undergoes a steady deepening, starting over northwestern Greenland at 12 UTC 18 September, and reaching

maximum strength of 979 hPa at 06 UTC 20 September, 6 hours after the snapshot shown in Figure 3b. Note that the NOGREEN low is not only some 15 hPa deeper than the primary low in CONTROL at this stage, but its path is shifted by about 4 degrees of latitude to the north, compared to CONTROL.

The weakening and southward shift of the primary low due to Greenland's orography are entirely consistent with the results of KRISTJÁNSSON and MCINNES (1999), who explained the weakening of the low by (i) the suppressed cold air advection behind the primary low due to orographic blocking of the cold air and (ii) warm air advection ahead of the secondary low, both of which reduce the baroclinic energy conversion of the primary low. PETERSEN et al. (2005) explained the southward displacement of lee lows (relative to the axis of symmetry) off Eastern Greenland by geostrophic adjustment, by which easterly flow toward the mountains enhances surface pressure to the north, while sinking warm air farther south induces low surface pressure there. Figure 4, which gives the difference in sea level pressure between CONTROL and NOGREEN illustrates this, showing a very distinct dipole between higher pressure to the north and lower pressure to the south. This figure is strikingly similar to Figure 6c in KRISTJÁNSSON and MCINNES (1999), for the 13 January 1995 case, suggesting that these features are quite characteristic manifestations of the influence of Greenland's orography on cyclone evolution, at least when the upper level flow is westerly.

In addition to the obstruction of the flow of cold air behind the developing baroclinic wave, our analysis suggests that in the present case also the warm air advection ahead of the low is similarly suppressed (not shown). An important part of the reason for these orographic flow distortions, which weaken the baroclinic development, is the large stability of the air impinging on Greenland in the autumn and winter. This means that the non-dimensional mountain height, or equivalently, inverse Froude number is rather large. Mathematically, it is defined as:

$$1/Fr = NH/U \qquad (4.1)$$

N being the Brunt-Vaisälä frequency, which is a measure of static stability, H being the mountain height and U the wind speed of the upstream flow. Typical values for the southerly flow on 19 September are $N \sim 0.01$ s^{-1}, $H \sim 3000$ m and $U \sim 10$ m s^{-1}. The inverse Froude number is then 3, and comparison with the regime diagram of SMITH (1989) and its extension to rotational flow by ÓLAFSSON and BOUGEAULT (1997) indicates that the conditions for blocking and flow splitting are favorable, so that strong lee effects should be expected. Sinking motion in the lee causes adiabatic warming, which creates a lee low at the surface. Here, it should be kept in mind that these theoretical considerations are based on the assumption of a wind speed and stability that are constant with height, but this should not affect the qualitative aspects of the argument. In NOGREEN, the flow of rising warm air is not blocked and it contributes to the baroclinic growth of the cyclone, in the same manner as the sinking cold air behind the low does.

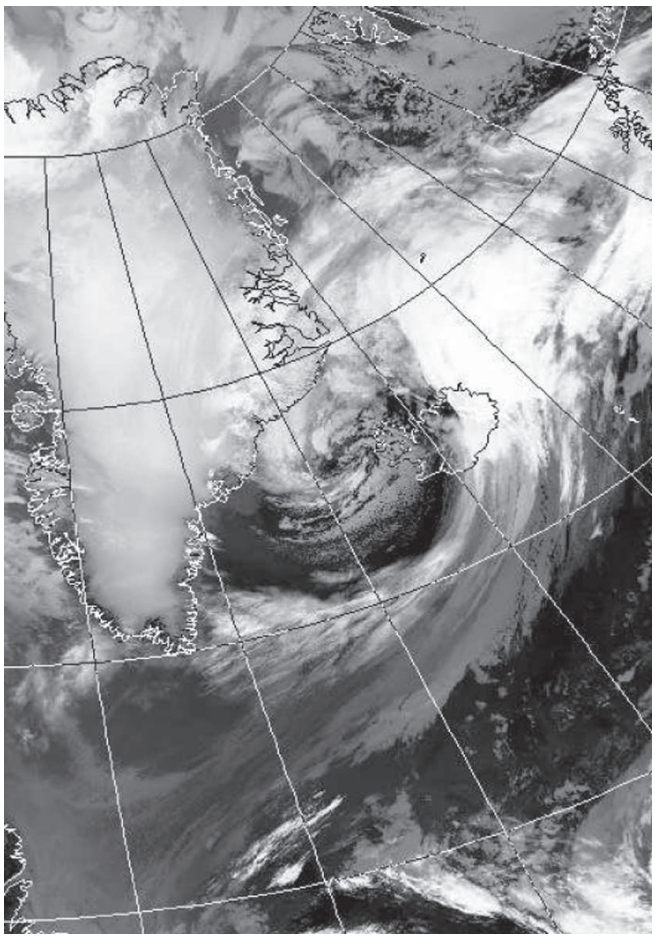

Figure 5: Infrared satellite picture at 13:39 UTC 20 September 2003 (obtained from Dundee Satellite Receiving Station).

In contrast to KRISTJÁNSSON and MCINNES (1999), the secondary low does not remain quasi-stationary. Instead, it intensifies rapidly as it starts to interact with the upper level trough approaching from the northwest (Figure 1a-d). At 06 UTC 20 September (+54 hours) the secondary low has turned into a major baroclinic disturbance with a low center at 66°N, 27°W and a well defined cold front, as seen by the satellite picture taken 7 $\frac{1}{2}$ hours later (Figure 5). The CONTROL run captures quite well the deepening phase of the secondary low, as seen by comparing Figure 3c to the analysis in Figure 2b. On the following day, the secondary low caused extreme weather conditions over northern Iceland, as northerly winds punched the north coast of Iceland, due to strong pressure gradients at the rear of the low (Figure 3e),

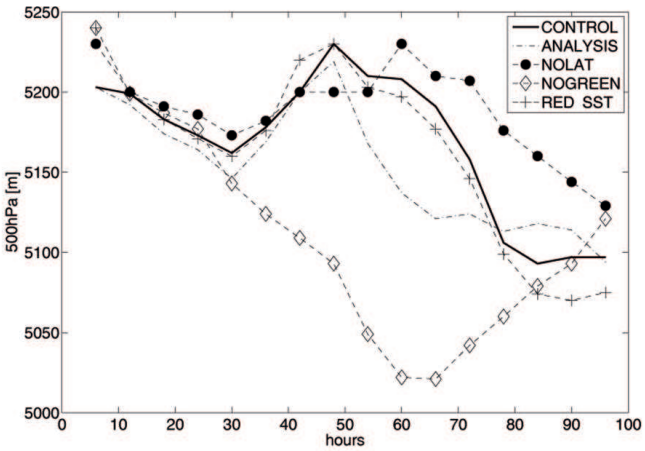

Figure 6: Minimum geopotential height associated with the cyclone development at 500 hPa [m] for the simulations and the analysis. The time axis runs from 00 UTC 18 September 2003.

creating blizzard conditions down to sea level. The secondary low in the CONTROL simulation reached maturity at 18 UTC 21 September with a central pressure of 973 hPa, 24 hours later than the low in the NOGREEN simulation (Figures 3d, 3f). Despite the vastly different cyclone evolutions in CONTROL and NOGREEN we note by comparing Figures 3e and 3f that as the low system moves farther away from Greenland, the difference between these two simulations is reduced.

As seen above and in Table 1 there are some differences in the evolution of the surface lows between the CONTROL simulation and the analysis. The primary low weakens more slowly in the CONTROL simulation than in the analysis. This leads to a delayed and less rapid intensification of the secondary low in CONTROL than in the analysis, but the main features of the situation are well captured. Figure 6 depicts the evolution of the trough at 500 hPa in the different model runs and the analysis. If we compare the CONTROL simulation to the analysis, we note that also at this level the trough at 500 hPa intensifies earlier and more rapidly in the analysis than in CONTROL. We further note how dramatically different the evolution in the NOGREEN run is, compared to all the other simulations. For instance, there is only one deepening event in the NOGREEN run, displaying a gradual, but strong deepening over the first 60 hours, while in all the other simulations, which have Greenland's orography in place, the height of the 500 hPa surface in the trough increases between 36 and 48 hours, followed by a new drop from 48 to 84 hours. The intermediate phase is associated with the southeastward crossing of Greenland, while in the final deepening phase the trough has turned into a strong upper level low (see Figure 1d), which is more and more phase-locked with the surface low.

4.2 PV considerations

To understand the interaction between the surface secondary low and the upper level trough, we have studied the evolution of potential vorticity (PV) at various levels and performed an inversion of selected PV anomalies, which provides a quantitative assessment of the contributions to the low-level pressure distribution from different parts of the atmosphere. The piecewise PV inversion is carried out under nonlinear balance conditions (DAVIS, 1992; KRISTJÁNSSON et al., 1999). The method is based on a partitioning of the total PV field into a time average and a perturbation field. The perturbation field consists of selected anomalies and a residual term. In this case, a 48 h time average is used, and the inversion of the PV anomalies is based on the ECMWF analysis fields available every 6 hours. The inversion is performed on pressure levels from 100 to 1000 hPa, with the lower boundary condition applied at 950 hPa and the upper boundary condition at 125 hPa (KRISTJÁNSSON et al., 1999). The following PV anomalies have been inverted:

1) The positive upper level PV anomaly moving across Greenland on 19–20 September (cf. Figure 1). It is defined between 600 hPa and 150 hPa. Its magnitude is 2–5 PV units (1 PV unit $\equiv$ 1 PVU = 10^{-6} K m^2 kg^{-1} s^{-1}).

2) A low level positive PV anomaly, that is located along the coast of eastern Greenland. It is defined between levels 900 and 700 hPa. This PV anomaly is quasi-stationary, due to lee effects associated with the persistent flow across Greenland, but its magnitude varies somewhat.

3) A low level positive potential temperature anomaly, defined at the 950 hPa level, covering much of Greenland before the onset of cyclogenesis, due to the warm southerly flow over the region on 19 September.

Concerning anomaly 3 it is important to keep in mind that a potential temperature anomaly at the lower boundary can be regarded as a PV anomaly of the same sign (HOSKINS et al., 1985).

At 06 UTC 19 September, about 24 hours before the secondary cyclone develops, the upper level PV anomaly is located over the west coast of Greenland (Figure 7a), and an interaction with the low level PV anomaly over the east coast appears unlikely, because of the intervening mountains and the large distance separating the two. This assertion is confirmed by Figure 8a, which shows that the 900 hPa geopotential height field associated with the upper level PV anomaly (blue contours) yields a fairly modest contribution to the depth

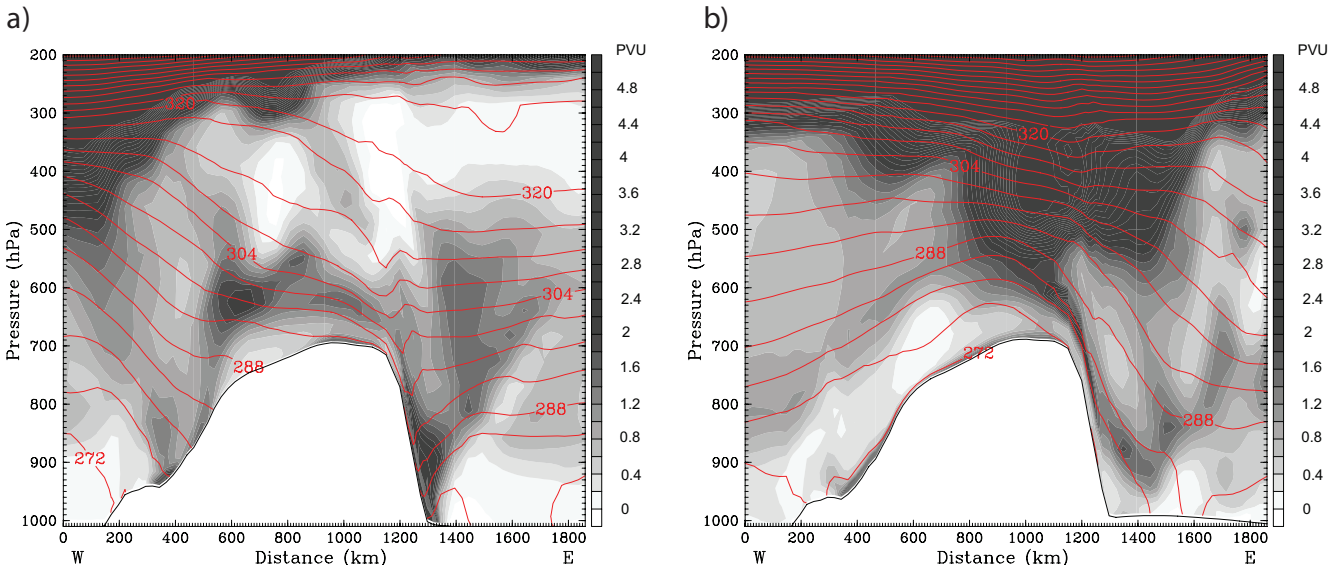

Figure 7: Cross sections (location marked in Figure 4) of potential vorticity [shading, PVU], and potential temperature [K]. Valid time: a) 06 UTC 19 September (+30 hours); b) 06 UTC 20 September (+54 hours).

of the incipient secondary cyclone, i.e., about –55 m. A similar contribution, i.e., about –40 m, is obtained from the lower tropospheric anomaly (black contours), but the largest contribution comes from the boundary-θ anomaly (red contours), which contributes about –70 m at this point in time. Figure 8a also shows the 900 hPa PV field (blue and green shading) itself, indicating a maximum value of about 2 PVU in exactly the location where the cross section in Figure 7a shows a zone of very high PV values extending from the surface to about 750 hPa. From this one may conclude that there is an ongoing production of low-level PV in the lee of southeastern Greenland in the early hours of 19 September, most likely caused by lee effects, i.e., vortex stretching and subsidence warming, as high-θ air is brought down toward the surface in the lee of the steep mountains. The flow is blocked and the θ-surfaces are collapsing, having a hydraulic jump-like structure, with PV generation through thermal diffusion tending to modify the potential temperature field following the flow so as to produce PV from vertical vorticity present in the jump (EPIFANIO and DURRAN, 2002).

Over the next 24 hours the upper level PV anomaly moves southeastward, and it gradually starts interacting constructively with the lower level PV anomaly. Consequently, the secondary low undergoes a rapid deepening, consistently with the theoretical considerations of HOSKINS et al. (1985). The vertical cross section from 06 UTC 20 September (Figure 7b) suggests that an interaction between the upper level PV anomaly and the secondary low at the surface is taking place. The results from PV inversion lend quantitative support to this assumption (Figure 8b): The surface-θ anomaly has now weakened, due to the lifting of the warm air and its subsequent wrapping around the developing cyclone. The secondary cyclone has now started developing (see e.g., Table 1) and we note that the main contribution comes from the upper level PV anomaly, reaching –280 m at 900 hPa at the cyclone center. This coincides with the downward extension of the upper level PV seen in Figure 7b, highlighting the coupling between the upper level PV anomaly and the low level cyclone development. The contribution from the lower troposphere is similar to what it was 24 hours earlier (Figure 8a). The stability is low, as indicated by nearly vertical θ-surfaces and this leads to a large Rossby scale height (H):

$$H = fL/N \tag{4.2}$$

(f being the Coriolis parameter and L a characteristic horizontal dimension), enabling the circulation associated with the upper level anomaly to penetrate down into the lower troposphere (HOSKINS et al., 1985). The connection between the upper level anomaly and the lower tropospheric anomaly thus spins up the circulation at all levels in the troposphere.

5 The secondary (lee) cyclone: A comparison of 2 cases

After this description of the cyclone evolution, there is one major question that remains to be answered: Why did the secondary low intensify explosively and move eastwards, instead of remaining a quasi-stationary lee-low as in KRISTJÁNSSON and MCINNES (1999).

In the January 1995 case of KRISTJÁNSSON and MCINNES (1999), the primary low was generated in a baroclinic zone south and southeast of Greenland. It

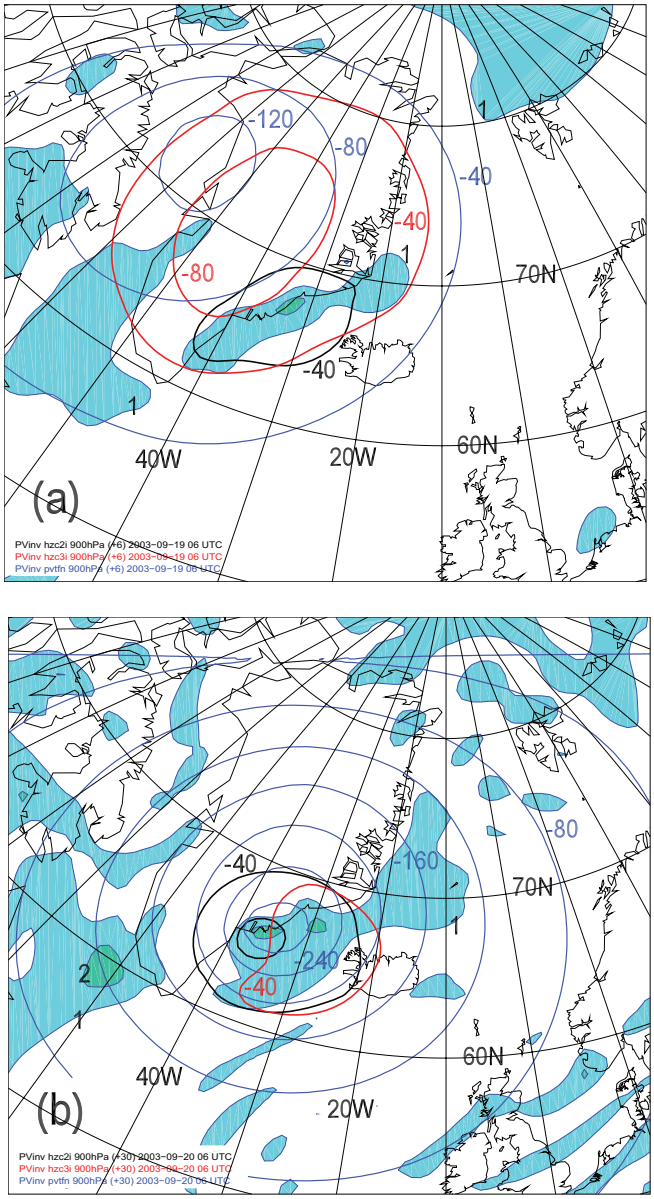

Figure 8: Contributions to geopotential height at 900 hPa (contour interval 40 m) from different PV anomalies, obtained by piecewise PV inversion. Blue contours refer to the upper level PV anomaly, black contours the lower tropospheric anomaly and red contours the lower boundary potential temperature anomaly. Shading denotes PV at the 900 hPa surface with contour interval 1 PVU. Valid time: a) 06 UTC 19 September; b) 06 UTC 20 September.

moved northeast along Greenland's east coast, and then split into two lows; a baroclinic low to the northeast and a secondary low generated by the mountains farther southwest. The primary low at the surface and the upper level low were always connected. In our September 2003 case the primary surface low quickly crossed Greenland from the northwest corner of Greenland. When it had reached the east coast of Greenland the upper level low was still located over the west coast of Greenland (Figure 1b). In between there is a 3000-meter high mountain and a distance of 1500 km, and hence a connection between the lows at lower and upper levels was not possible. Instead it was the secondary low that connected with the upper level trough after the latter had moved across Greenland. That is why the secondary low intensified, while the primary low, without support from upper levels and with unfavorable conditions for temperature advection, rapidly weakened and filled.

6 Results from the other simulations

In the lower troposphere, excluding latent heating (NOLAT) weakens both the primary and the secondary low, as expected (Table 1). This weakening gradually increases and reaches respectively +12 hPa at 60 hours for the primary low and +18 hPa at 90 hours for the secondary low. This means that latent heating is responsible for about half of the deepening of the secondary cyclone. For the 500 hPa trough (Figure 6) the importance of latent heating is quite small during the first 48 hours, because the 500 hPa trough is decoupled from the surface (primary) low. After 60 hours, however, the 500 hPa trough becomes phase locked with the surface (secondary) low and a larger sensitivity to latent heating is found.

Reducing SST by 5 K did not have much impact on the course of events. There was a general pressure rise over the oceans due to the lower surface temperature, and this affected both the primary and secondary lows, rendering them a few hPa weaker in REDSST than in the CONTROL run (Table 1).

7 Conclusions

Simulations and PV diagnostics of a cyclone that caused a severe winter storm on 20–21 September 2003 in eastern Greenland and northern Iceland have revealed the following course of events: In the aftermath of a baroclinic development that was greatly suppressed by Greenland's orography, a secondary lee-cyclone was formed between Iceland and Greenland. The secondary cyclone deepened explosively as it interacted with an upper-level PV anomaly that approached from the northwest. The severe weather occurred in connection with the bent-back front at the rear of the cyclone as it moved east-northeast.

Compared to previous studies of Greenland's influence on cyclone developments, in particular the study by KRISTJÁNSSON and MCINNES (1999), the results here contain interesting similarities and differences. In both cases the initial (primary) cyclone development near Greenland's east coast was greatly hampered by the presence of Greenland's orography, and in both cases a secondary (lee) cyclone was formed near 66°N, 35°W. However, whereas the secondary cyclone

remained quasi-stationary without developing significantly in the January 1995 case of KRISTJÁNSSON and MCINNES (1999), its counterpart underwent explosive deepening in the case studied here, turning into a major baroclinic disturbance which moved east-northeast, causing hurricane-force winds and heavy snowfall associated with its bent-back front. The difference between the two cases is related to differences in the interaction between the lower and upper troposphere: In the present case, the primary low moved rapidly eastwards across Greenland, while the upper level disturbance moved very slowly, and hence there was no interaction between the two, causing this low to weaken rapidly. Subsequently, when the upper level disturbance approached Greenland's east coast, the secondary low was in a favorable position to interact with it, and an explosive development took place. Conversely, in the January 1995 case the low-level secondary low was merely an orographic feature, not supported by any upper level disturbance. This study suggests that forecasts of severe weather in Iceland can be extremely sensitive to orographic forcing of Greenland, even on time scales of ~ 1 day. Successful forecasts require an adequate treatment of orographic blocking, and a good observational data coverage in the region.

References

DAVIS, C. A., 1992: Piecewise potential vorticity inversion. – J. Atmos. Sci. **49**, 1397–1411.

DOYLE, J. D., M. A. SHAPIRO, 1999: Flow response to large scale topography: the Greenland tip jet. – Tellus, **51A**, 728-748.

EPIFANIO, C. C., D. R. DURRAN, 2002: Lee-vortex formation in free-slip stratified flow over ridges. Part II: Mechanisms of vorticity and PV production in nonlinear viscous wakes. – J. Atmos. Sci. **59**, 1166–1181.

GRELL, G. A., J. DUDHIA, D. R. STAUFFER, 1995: A description of the fifth-generation Penn State/NCAR Mesoscale Model (MM5). – NCAR Tech. Note NCAR/TN-398 + STR, 122 pp.

HOSKINS, B. J., M. E. MCINTYRE, A. W. ROBERTSON, 1985: On the use and significance of isentropic potential vorticity maps. – Quart. J. Roy. Meteor. Soc. **111**, 877–946.

JUNGE, M. M., R. BLENDER, K. FRAEDRICH, V. GAYLER, U. LUKSCH, F. LUNKEIT, 2005: A world without Greenland: impacts on the Northern Hemisphere winter circulation in low- and high-resolution models. – Climate. Dyn. **24**, 297–307.

KLEIN, T., G. HEINEMANN, 2002: Interaction of katabatic winds and mesocyclones near the eastern coast of Greenland. – Meteor. Appl. **9**, 407–422.

KRISTJÁNSSON, J. E., H. MCINNES, 1999: The impact of Greenland on cyclone evolution in the North Atlantic. – Quart. J. Roy. Meteor. Soc. **125**, 2281–2834.

KRISTJÁNSSON, J. E., S. THORSTEINSSON, G. F. ULFARSSON, 1999: Potential vorticity-based interpretation of the evolution of the 'Greenhouse Low', 2–3 February 1991. – Tellus **51A**, 233–248.

KURZ, M., 2004: On the dynamics of the splitting process of cyclones near southern Greenland. – Meteorol. Z. **13**, 143–148.

MM5 USER'S GUIDE, 2001: PSU/NCAR Mesoscale Modeling System Tutorial Class Notes and User's Guide: MM5 Modeling System Version 3, PSU/NCAR, 300 pp.

MOORE, G. W. K., I. A. RENFREW, 2005: Tip jets and barrier winds: A QuikSCAT climatology of high wind speed events around Greenland. – J. Climate **18**, 3713–3725.

ÓLAFSSON, H., 1998: Different predictions by two NWP models of the surface pressure field east of Iceland. – Meteor. Appl. **5**, 253–261.

ÓLAFSSON, H., P. BOUGEAULT, 1997: The effect of rotation and surface friction on orographic drag. – J. Atmos. Sci. **54**, 193–210.

PETERSEN, G. N., H. ÓLAFSSON, J. E. KRISTJÁNSSON, 2003: Flow in the lee of idealized mountains and Greenland. – J. Atmos. Sci. **60**, 2183–2195.

PETERSEN, G. N., J. E. KRISTJÁNSSON, H. ÓLAFSSON, 2004: Greenland and the Northern Hemisphere winter circulation. – Tellus, **56A**, 102–111.

—, —, —, 2005: The effect of upstream wind direction on atmospheric flow in the vicinity of a large mountain. – Quart. J. Roy. Meteor. Soc. **131**, 1113–1128.

PICKART, R. S., M. A. SPALL, M. H. RIBERGAARD, G. W. K. MOORE, R. F. MILLIFF, 2003: Deep convection in the Irminger Sea forced by the Greenland tip jet. – Nature **424**, 152–156.

SCHWIERZ, C. B., H. C. DAVIES, 2003: Evolution of a synoptic-scale vortex advecting toward a high mountain. – Tellus **55A**, 158–172.

SCORER, R. S., 1988: Sunny Greenland. – Quart. J. Roy. Meteor. Soc. **114**, 3–29.

SMITH, R. B., 1989: Hydrostatic airflow over mountains. – Adv. Geophys. **31**, 1–41.